Article

Establishment and application of continuous real–time release model for storage tank

Juanxia He[1, 2*], Liliang Yang[2], Angang Li[2], Qiyong Zhou[2], Dongmei Zhou[2], Lei Liu[2], Daping Yang[3], Yongzhong Zhan[1, 2*]

1 School of Materials Science and Engineering, South China University of Technology, Guangzhou 510641, China; hejuanxia2005@126.com (J. He); zyzmatres@aliyun.com (Y. Zhan)

2 . School of Resources, Environment and Materials, Guangxi University, Nanning 530004, China; 1769435135@qq.com (L. Yang); 972151003@qq.com (A. Li); 2304580956@qq.com (Q. Z.); 1003810227@qq.com (D. Z.); 974227654@qq.com (L. L.)

3. Department of Civil Engineering, Guangxi Polytechnic of Construction, Nanning 530007, China; 245407863@qq.com (D. Yang)

* Corresponding authors: E–mail: hejuanxia2005@126.com (J. He), zyzmatres@aliyun.com (Y. Zhan)

Abstract: The calculation of the release of liquid hazardous chemicals storage tanks is an important part of the quantitative risk assessment of accidents. This paper mainly establishes a continuous real–time release model based on the instantaneous mass flow Q_m model. Meanwhile, the software function module was analyzed, and programming software was developed using *C#* language for model solving. A series of experiments for repeated leakage tests was designed and the discharges through three small holes with different heights for 200 s were observed. The results show that the continuous real–time leakage model is effective, and the deviation between theoretical and experimental release amounts are within a reasonable range. The higher the liquid level above the leak hole is, and the smaller the height of the leak hole from the ground is, the greater the flow rate at the leak orifice is and the smaller discharge rate change is. Therefore, the deviation between the theoretical release amount M_t and the experimental average release amount M_a is greater while the height of the leak hole from the ground is smaller, which indicates that the smaller the distance from the leak orifice to the ground, the greater the influence of the empirical discharge coefficient C_0 on the release amount M.

Key words: storage tank; continuous real–time; release model; leakage test; hole discharge

---

1. Introduction

The storage tanks are used to store high-energy material like liquid chemical. Release from a liquid hazardous chemical storage tank occurred if the steel storage tank was improperly maintained, gradually corroded or suddenly cracked [1]. Incidents including fire and explosion or poisoning and suffocation caused major casualties and property losses when the released liquid evaporated and reached a certain concentration [2–4]. Committee for Prevention of Disaster published some guidelines to identify, analyze, calculate and evaluate incidental releases of hazardous materials of pipelines, tanks and pressure containers, by using quantitative risk assessment and qualitative risk assessment [5–7]. In previous research, scholars have studied the quantitative and qualitative risks about tank accidents. For instance, CFD software was used to simulate and analyze the catastrophic dyke overflow accident of oil tanks, and obtain the impacting factors including tank volume, the height of the fire dam, the nature of the oil, the arrangement of the tank group, and rupture patterns [8]. Luo et al. carried out comprehensive study for the failure probability of tank leakage level by fishbone diagram and risk matrix analysis method, which can mitigate the risk of accidents [9]. A model was used to study the dynamic process of oil leakage in a double–hull oil tanker [10]. Probabilistic method was used to analyze hazardous chemical spills, establish a quantitative risk assessment model, determine acceptable risk levels, and evaluate tanks in an industrial park [11]. The accidental release of long–distance pressurized oil pipelines was analyzed, the model to calculate accumulated volume was obtained, and finally its practicality and accuracy was testified by experiments [12]. These researches of predecessors provide the references to resolve the continuous real–time release model for storage tank in this paper.

At present, the quantitative risk assessment of tank leakage accidents is characterized by the multiplication of the possible consequences of the accident and the frequency of accidents [5–7, 13]. The possible consequences of the accident are the basis for studying the risk of the accident, and the consequence calculation of the quantitative risk accident was closely related to the release of toxic and hazardous substances in the accident [12, 14–15]. The leakage analysis for vertical tank was estimated by instantaneous mass flow rate or Bernoulli equation [16–17]. However, the accuracy of the liquid level gauge used in industrial tanks is shown at millimeter level. When the valve of inlet/outlet is closed, the liquid storage tank is in a relatively static state [18]. Once the manual safety inspection in the tank area is not fulfilled timely or the flammable and explosive toxic gas detector fails, the leakage amount from the tank liquid dropping level is difficult to be assessed [19], especially for a large–capacity storage tank (such as an internal floating tank, volume V = 50000 m^3, diameter D = 60 m, tank height H = 19.44 m; when the liquid level drops by 1 mm, the leaked liquid is about 2.827 m^3).

This study mainly focuses on the relationship between continuous real–time release amount M and leakage time t of liquid hazardous chemicals vertical tank, and the model of M to solve the practical engineering problem of tank leakage calculation is obtained, which provides an effective solution for enterprise safety management and accident prevention.

2. Mathematical Modeling

2.1. Instantaneous Mass Flow Model

In the existing standard "Guidelines for Quantitative Risk Assessment of Chemical Enterprises" [20] (China Coal Industry Publishing House, 2013), the instantaneous mass flow that the leakage liquid flows out through the holes of the storage tank is calculated by equation (1):

$$Q_m = \rho \times A \times C_0 \times \sqrt{2 \times \left(\frac{P\text{-}P_0}{\rho} + g \times h_L \right)} \tag{1}$$

The leakage of a certain leak time period is generally calculated by using the instantaneous mass flow at the initial moment of the leak and the leak time, however, the liquid level h_L (above the leak hole in the tank) changes with the leak time t, which causes the instantaneous mass flow Q_m to change accordingly when the tank leaks continuously. As a result, this method can not calculate the true continuous leakage amount M accurately during the leakage time period.

In order to achieve the fundamental goal of early warning and prevention, and realize the development of emergency response plans, it is an urgent need to establish a relationship model between the continuous real–time release amount M and the leakage time t.

2.2. Model Building

During the service period, corrosive ions in the hazardous chemicals solution cause corrosion to the inner wall of the storage tank, while corrosive medium in the atmosphere cause corrosion to the outer wall of the storage tank [21–22]. Under these conditions, the wall of the storage tank became locally thinned, therefore there may be a pitting hole on the wall and the surface breaks and leakage occurs because the sudden pressure drops at the wall after a certain time [23–25]. As a result, the two major factors affecting the continuous real–time leakage are the falling height of the liquid level in the tank and the flow speed of the liquid at the leaking hole. Basing on these two factors, the mathematical modeling process for real–time leakage is shown in Figure 1. The schematic diagram of tank leakage is shown in Figure 2.

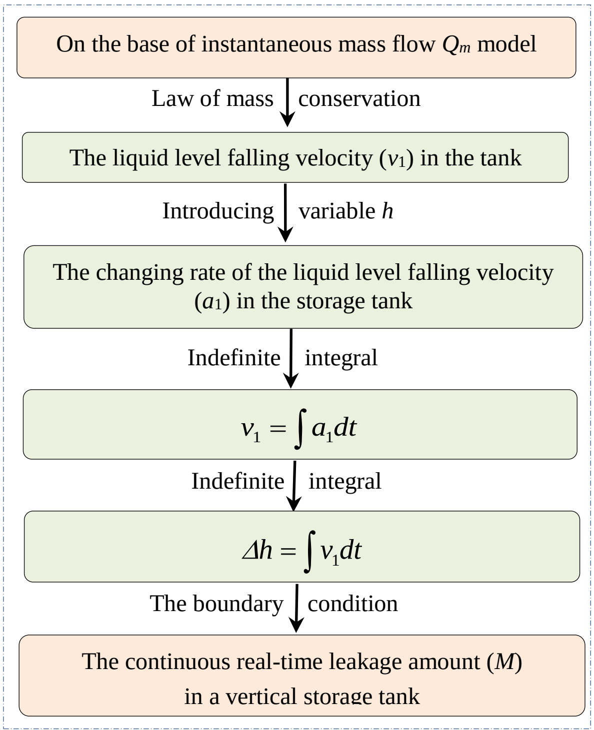

Figure 1. Mathematical modeling flow chart.

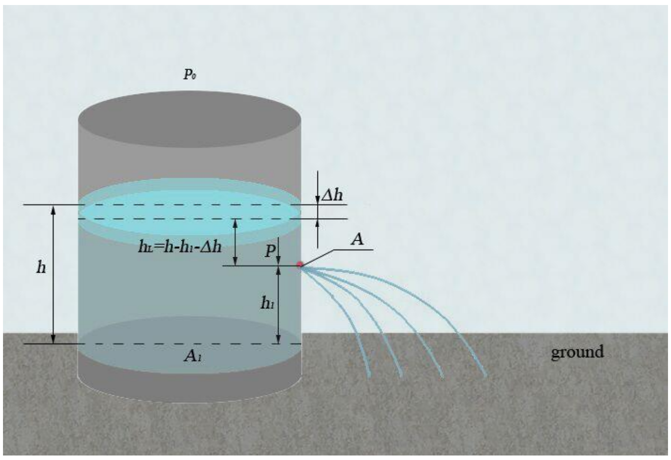

Figure 2. Schematic diagram of tank leakage.

2.2.1. Liquid Level Falling Velocity

The liquid level in the tank is continuously decreasing when leakage occurs. The falling liquid level velocity (v_1) in the tank could be characterized with the height of the liquid that is higher than the leaking point (h_L).

The liquid flow velocity v at the leak point is firstly investigated and characterized with h_L. At the leaking point by the principle of mass conservation :

$$Q_v = \frac{Q_m}{\rho} \tag{2}$$

$$Q_v = A \times v \tag{3}$$

Equation (2) and Equation (3) are combined with Equation (1), thus the liquid flow rate (v) at the leak point would be:

$$v = C_0 \times \sqrt{2 \times \left(\frac{P\text{-}P_0}{\rho} + g \times h_L \right)} \tag{4}$$

According to the basic law of conservation of mass, the quality of the liquid dropping in the tank should be the same as that of the leaking–out liquid through the leaking point:

$$\rho \times A \times v = \rho \times A_1 \times v_1 \tag{5}$$

Then the liquid level falling velocity (v_1) in the tank could be obtained by Equations (4) and (5):

$$v_1 = \frac{A}{A_1} \times C_0 \sqrt{2 \times \left(\frac{P\text{-}P_0}{\rho} + g \times h_L \right)} \tag{6}$$

2.2.2. Changing Rate of the Liquid Level Falling Velocity

The changing rate of the liquid level falling velocity is dependent on several factors, such as the diameter and height of the storage tank, the height of the liquid level in the storage tank, and the diameter of the leaking hole.

The change in the liquid level above the leaking point is taken into account for the leakage at any weak part of the tank:

$$h_L = h - h_1 - \Delta h \tag{7}$$

Equation (6) is squared, and combined with (7), then the solution would be:

$$\Delta h = \frac{\left(\frac{p\text{-}p_0}{\rho} + g \times h\text{-}g \times h_1 \right)}{g} - \frac{v_1^{\,2}}{2\left(\frac{A}{A_1} \times C_0 \right)^2 \times g} \tag{8}$$

Assuming that the leakage time is t, and the liquid level drop height Δh in the tank is found derivation for v_1:

$$\frac{d\Delta h}{dv_1} = \frac{d\Delta h}{dt} \times \frac{dt}{dv_1} = \frac{v_1}{a_1} \tag{9}$$

$$\frac{d\,\Delta h}{dv_1} = -\frac{v_1}{\left(\frac{A}{A_1} \times C_0 \right)^2 \times g} \tag{10}$$

The changing rate of the liquid level falling velocity in the storage tank is solved by the Equations (9) and (10):

$$a_1 = -\left(\frac{A}{A_1} \times C_0\right)^2 \times g \tag{11}$$

2.2.3. Continuous Real–time Release Model M

The liquid level falling velocity (v_1) is obtained via indefinite integral of the leak time by the changing rate of the liquid level falling velocity in the storage tank (a_1):

$$v_1 = \int a_1 \times dt = -\int g \times \left(\frac{A \times C_0}{A_1}\right)^2 \times dt = -\left(\frac{A \times C_0}{A_1}\right)^2 g \times t + C_1 \tag{12}$$

The integral constant C_1 is found by the boundary condition (t = 0, v_1 is the maximum value, and Δh is zero), so:

$$C_1 = \frac{A \times C_0}{A_1} \times \sqrt{2 \times \left[\frac{P - P_0}{\rho} + g \times (h - h_1)\right]} \tag{13}$$

The liquid level falling velocity (v_1) is obtained by Equations (12) and (13):

$$v_1 = \frac{A \times C_0}{A_1} \sqrt{2 \times \left[\frac{P\text{-}P_0}{\rho} + g \times (h\text{-}h_1)\right]} \times \left(\frac{A \times C_0}{A_1}\right)^2 \times g \times t \tag{14}$$

The liquid level drop height (Δh), as in the integral to the leak time t, could be characterized with the liquid level falling velocity (v_1):

$$\Delta h = \int v_1 dt = \frac{A \times C_0}{A_1} \sqrt{2 \times \left[\frac{P\text{-}P_0}{\rho} + g \times (h - h_1)\right]} \times t - \frac{g \times t^2}{2}\left(\frac{A \times C_0}{A_1}\right)^2 + C_2 \tag{15}$$

The integral constant C_2 is found by the boundary condition, if t = 0 and Δh = 0, then C_2 = 0, and:

$$\Delta h = \frac{A \times C_0}{A_1} \sqrt{2 \times \left[\frac{P\text{-}P_0}{\rho} + g \times (h - h_1)\right]} \times t - \frac{g \times t^2}{2}\left(\frac{A \times C_0}{A_1}\right)^2 \quad (\Delta h \le h - h_1) \tag{16}$$

In summary, the continuous real–time leakage amount M of the vertical tank body is obtained under the condition of $M = \rho V = \rho A_1 \Delta h$:

$$M = \rho \times A \times C_0 \sqrt{2 \times \left[\frac{P\text{-}P_0}{\rho} + g \times (h - h_1)\right]} \times t - \frac{\rho \times g \times C_0^{\,2} \times A^2}{2 \times A_1} \times t^2 \quad (\Delta h \le h - h_1) \tag{17}$$

2.3. Model Constraints and Verification

The model constraints of the continuous real–time leakage model M are as follows:

(1) Before the time that the tank leakage occurs, that is, the leakage time $t_{\text{leakage start}}$ = 0, the liquid level falling height $\Delta h_{\text{start}} = h - h_1 = 0$ and the continuous true leakage amount $M_{\text{start}} = 0$;

(2) When the leakage is completed (all liquid above the leak orifice flows out), that is, when the $t_{\text{leakage end}}$ reaches at a certain time, the liquid level descending height $\Delta h_{\text{start}} = h - h_1$ and the continuous true leakage amount $M_{\text{end}} = M_{\max}$.

(3) During any time period [t_i, t_{i+1}], $0 \le M_i < M_{i+1}$.

According to the actual liquid leakage and the model analysis, if the model constraints are established for the continuous real–time leakage amount calculation with the time *t* as the variable, the model is effective.

3. Model Application

3.1. Model of Software Construction

C# language is used to develop the corresponding software in order to facilitate the model solving and application. After the software functions are analyzed, the model input parameters and their logical relationships are determined, as well as the calculation output results and the graphic display functions, and the software programming is completed. Figure 3 shows the software development flow chart. Figure 4 shows the software application interface, (a) and (c) of Figure 4 are the whole process simulation amount, (b) and (d) of Figure 4 are the simulation amount of 200 s when the discharge coefficient is 0.65 and 0.82 respectively under the experimental application.

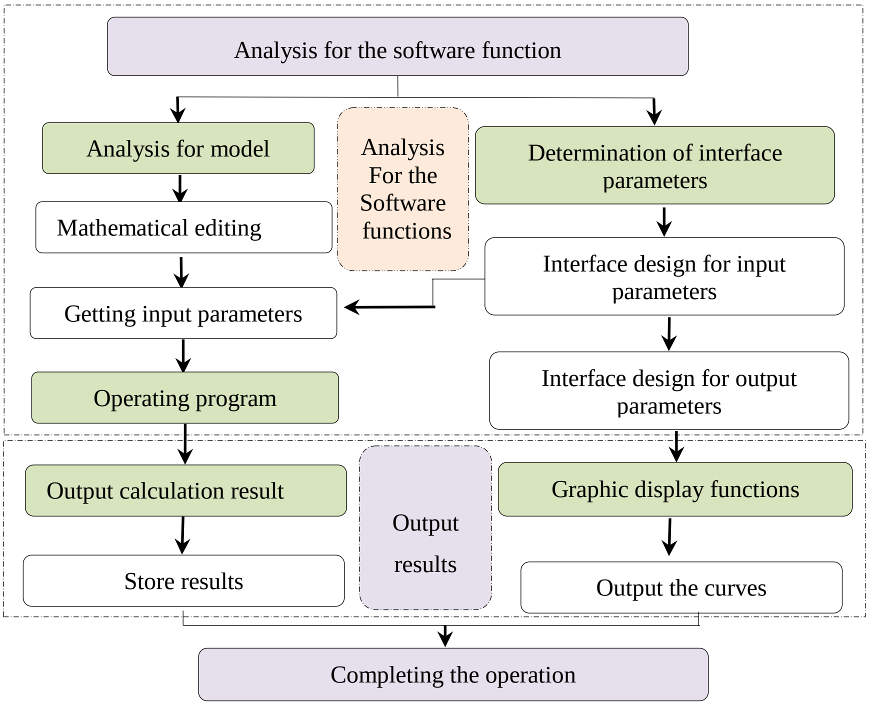

Figure 3. Software development flow chart.

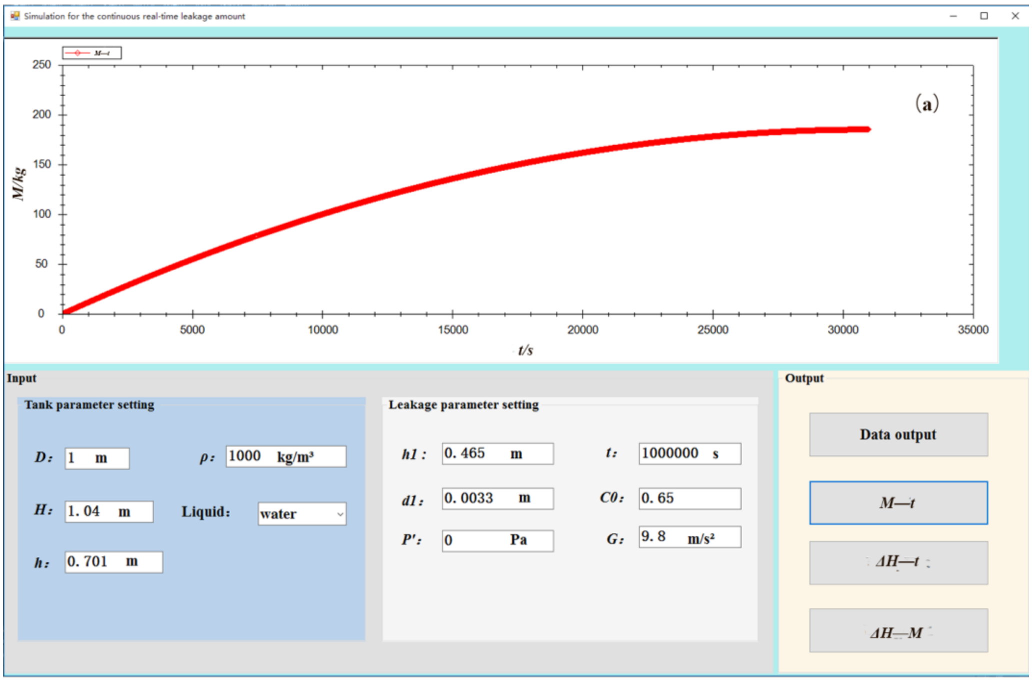
Simulation for the continuous real-time leakage amount
M—t
(a)
M/kg
t/s
0
50
100
150
200
250
0
5000
10000
15000
20000
25000
30000
35000
Input
Tank parameter setting
D: 1 m
ρ: 1000 kg/m³
H: 1.04 m
Liquid: water
h: 0.701 m
Leakage parameter setting
h1: 0.465 m
t: 1000000 s
d1: 0.0033 m
C0: 0.65
P′: 0 Pa
G: 9.8 m/s²
Output
Data output
M—t
ΔH—t
ΔH—M

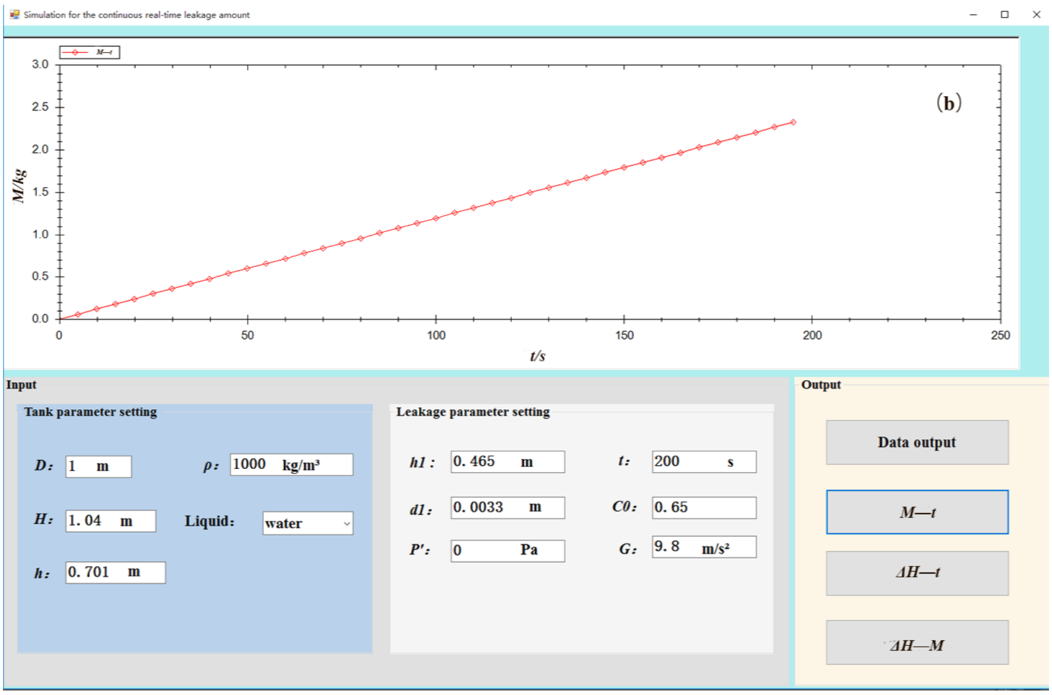
Simulation for the continuous real-time leakage amount
M—t
(b)
M/kg
t/s
0.0
0.5
1.0
1.5
2.0
2.5
3.0
0
50
100
150
200
250
Input
Tank parameter setting
D: 1 m
ρ: 1000 kg/m³
H: 1.04 m
Liquid: water
h: 0.701 m
Leakage parameter setting
h1: 0.465 m
t: 200 s
d1: 0.0033 m
C0: 0.65
P′: 0 Pa
G: 9.8 m/s²
Output
Data output
M—t
ΔH—t
ΔH—M

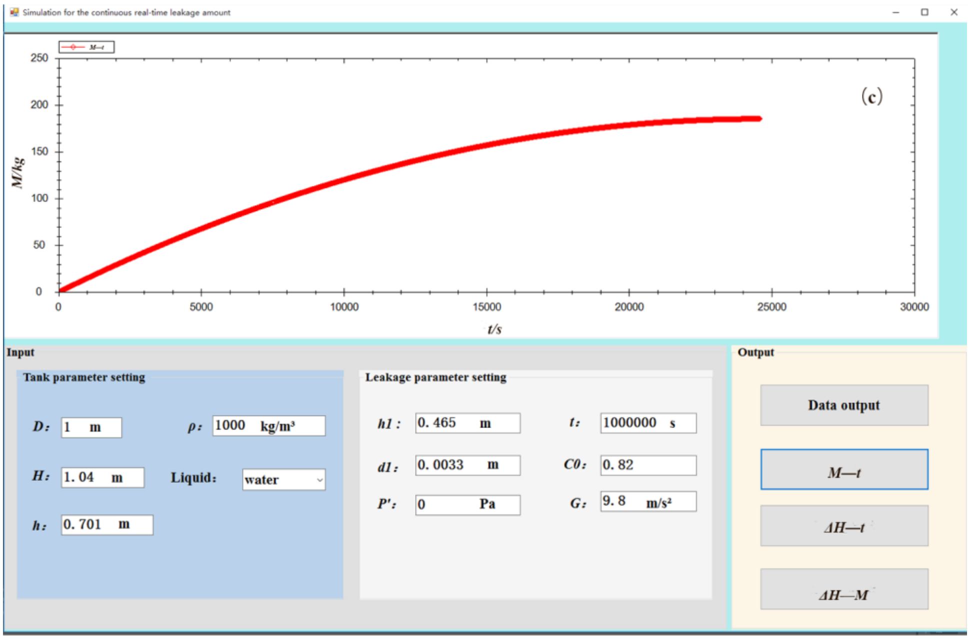

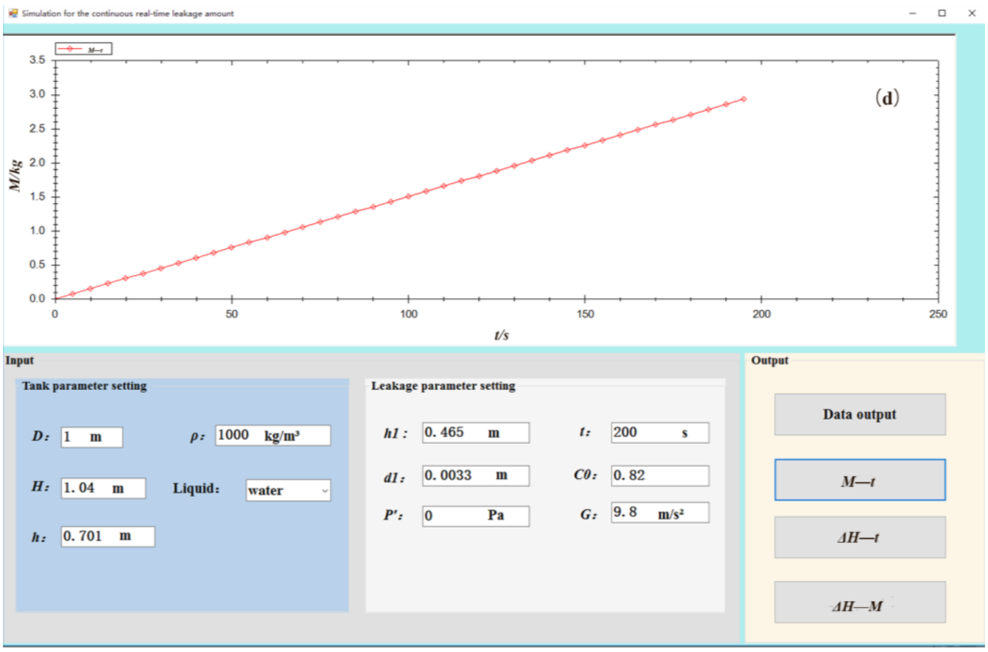

Figure 4. Software application interface.

3.2. Experimental Application

3.2.1. Leakage Tanks and Main Parameters

A tank was specifically designed and tested in order to evaluate the application of the model and the operation of the software. The storage tank was made of PVC material and was a flat–bottom cylindrical storage tank. The diameter of the bottom is D = 0.98 m, the total height is H = 1.45 m, and the height of the cylindrical part is H_1 = 1.04 m. The simulated leakage is through the small round holes. A plumb line was taken with a steel ruler and a level meter, and the position of the leak holes was calibrated from bottom up. The leakage hole diameter d was measured by averaging three measurements using vernier caliper at three different angles through circle center. The leakage hole diameter d, the distance from the leaking point to tank bottom h_1, the initial liquid level height h, and the leakage hole shape are shown in Table 1.The leaking test liquid is tap water.

Table 1. Data sheet of tank leakage Information.

hole number	*h*/m	h_1/m	shape of leakage hole	*d*/m
1	0.701	0.617	circular	0.0033
2	0.701	0.4677	circular	0.0034
3	0.701	0.2677	circular	0.0034

The discharge coefficient C_0 of 0.65 was generally applied for a circular leak hole, which was introduced in the book about accident analysis [26]. C_0 was not a clear value when tank body leaked in AQ3046–2013. However it was clearly stated that the discharge coefficient was 0.62 for sharp orifices, 0.82 for rounded orifices, and 0.96 for straight orifices. So the theoretical values of C_0 are 0.65 and 0.82 to be compared with experimental value [7].

3.2.2. Experiment Requirement

Three repeated experiments were performed for each leak hole to better analyze the experimental results. A pressure sensing liquid level gauge was added to the test to facilitate real–time measurement of the leakage amount and real–time change of the liquid level. The relationship between the leakage time t and the real–time discharge amount M within a certain leakage period according to the simulation results of the model needs to be verified.

The leakage time step is 5 s during the experiments. The leaking liquid is collected and weighed in a 1000 mL beaker for 200 s. The leaking experiment site is shown in Figure 5.

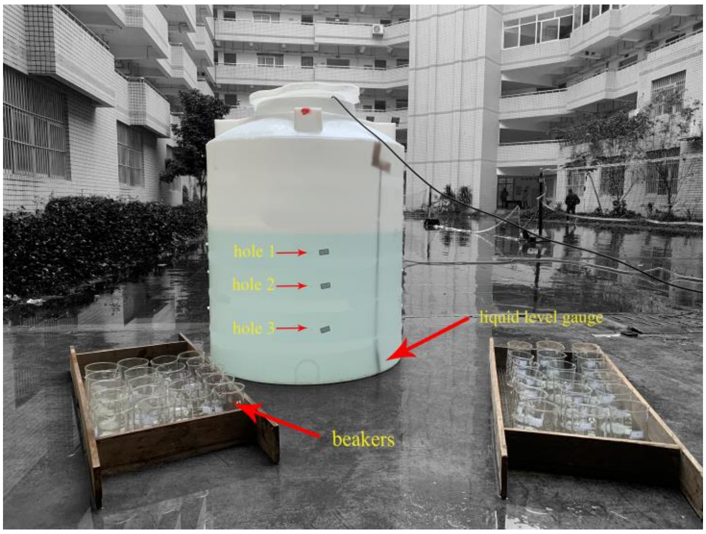

Figure 5. Leaking experiment site.

4. Experimental Results and Discussion

4.1. Experimental Results

Each leakage orifice of No.1, No.2 and No.3 is tested for three times, and the discharge amount of every time step is collected, weighted and recorded. Then every graph of three real–time leakage amounts M_1, M_2 and M_3 are obtained. Then Figure 6, Figure 7 and Figure 8 illustrate the leakage amount of hole 1, 2, and 3 on time respectively. Figure 6 shows that M_1, M_2 and M_3 of hole 1 (d = 0.0033 m, h = 0.701 m and h_1 = 0.617 m) are close to each other, especially for the first two experiments, and the graph of M_1 is the largest among three discharging experiments. The amount of M_1 M_2 and M_3 is 1783.88 g, 1760.22 g and 1657.20 g respectively when the leakage time is 200 s. Figure 7 shows that M_1, M_2 and M_3 of hole 2 (d = 0.0034 m, h = 0.701 m and h_1 = 0.4677 m) are nearly the same, especially for the first two experiments, and the graph of M_2 is the largest among three discharging experiments. The amount of M_1 M_2 and M_3 is 2967.12 g, 3043.92 g and 2836.91 g respectively when the leakage time is 200 s. Figure. 8 shows that M_1, M_2 and M_3 of hole 3 (d = 0.0034 m, h = 0.701 m and h_1= 0.2677 m) have almost no deviation, and the graph of M_2 is the largest among three discharging experiments. The amount of M_1 M_2 and M_3 is 4034.18 g, 4105.14 g and 4065.25 g respectively when the leakage time is 200 s.

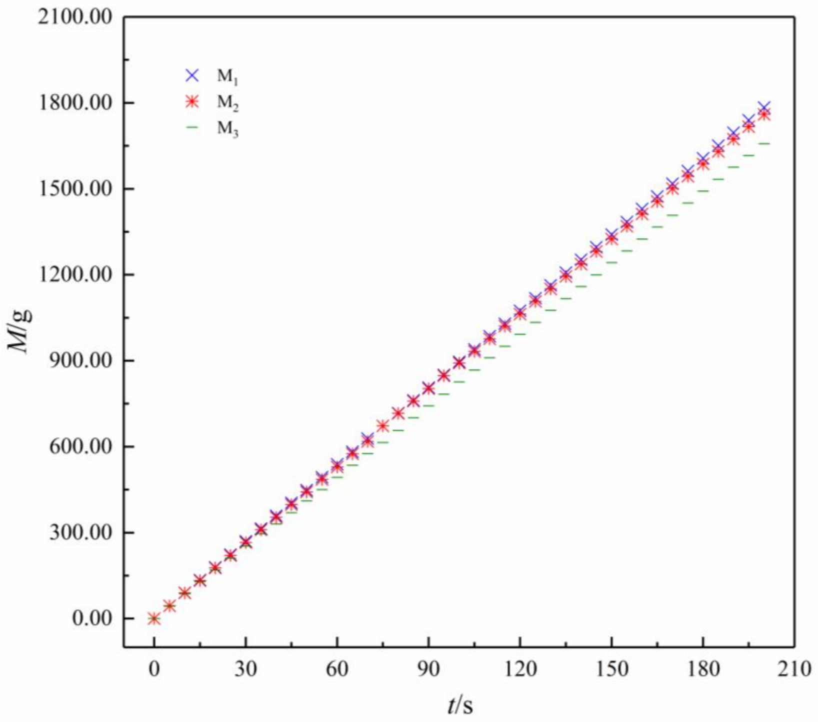

Figure 6. Leakage amount curves of hole 1 with time (d = 0.0033 m, h = 0.701 m and h_1 = 0.617m).

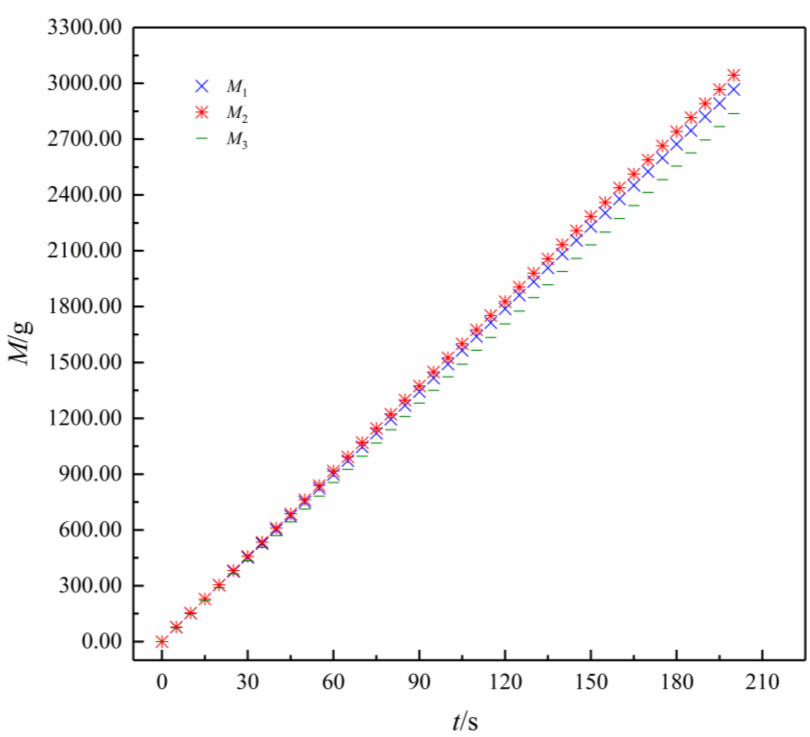

Figure 7. Leakage amount curves of hole 2 with time (d = 0.0034 m, h = 0.701 m and h_1 = 0.4677m).

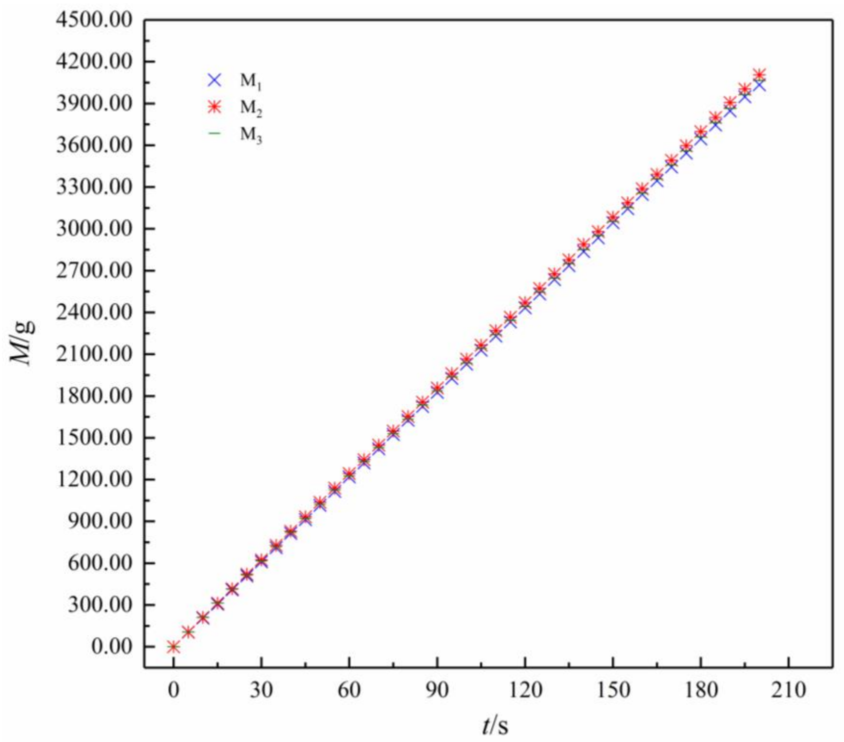

Figure 8. Leakage amount curves of hole 3 with time (d = 0.0033 m, h = 0.701 m and h_1 = 0.2677m).

Figure 9 shows the structure of liquid level sensor. The actual liquid level differs by 5.5 cm since the pressure sensing element is 5.5 cm from the bottom of the liquid level gauge. Figure 10 reveals the relationship between the liquid falling level and the leakage time. The liquid level gauge shows that once the leakage occurs, the leakage amount cannot be judged based on the change of the level gauge's readings.

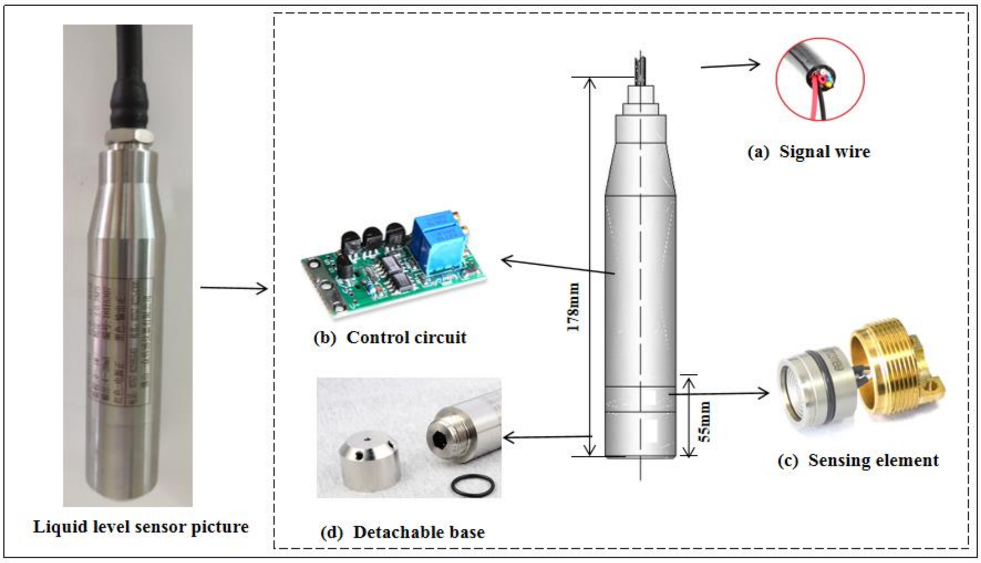

Figure 9. Structure of liquid level sensor.

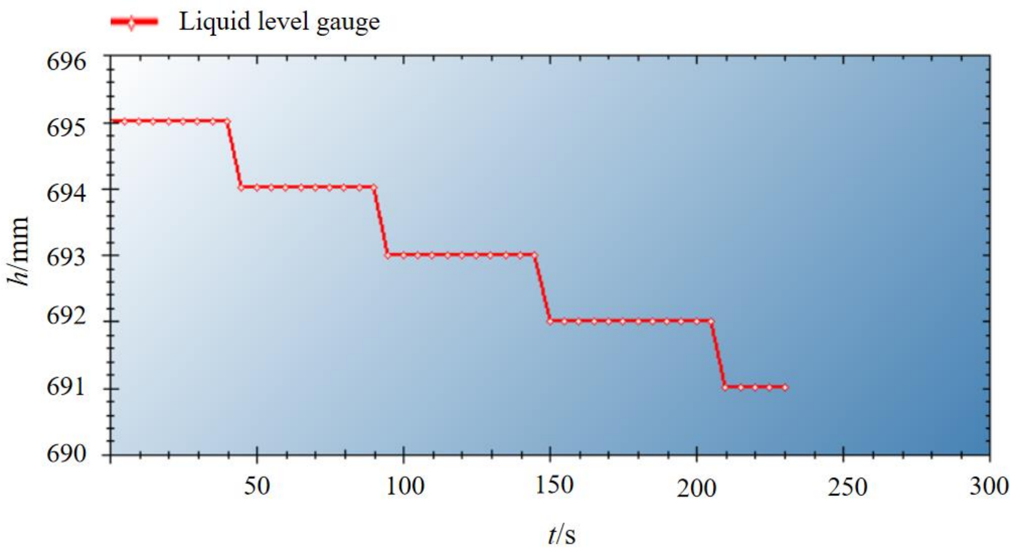

Figure 10. Relationship between liquid level drop and leakage time.

4.2. Discussion

4.2.1. Comparative Analysis of Leakage

The average amount M_a from three measurements of every discharging experiments is obtained to make a straightforward comparison. The positive deviation of the average by 20 % ($M_{a+20\%}$), the negative deviation of the average by 20 % ($M_{a-20\%}$), and the theoretical leakage amount $M_{t0.65}$ (when $C_0 = 0.65$) and $M_{t0.82}$ (when $C_0 = 0.82$) are illustrated in Figure 11, Figure 12 and Figure13. M_a and M_t are in the intervals of $M_{a+20\%}$ and $M_{a-20\%}$ for hole 1, hole 2 and hole 3. Figure 11 shows that M_a, with the releasing time of 200 s, is much larger than $M_{t0.65}$ but much closer to $M_{t0.82}$, and $M_{t0.65}$ is very close to $M_{a-20\%}$ when the tank body is continuously released by hole 1 (d = 0.0033 m, h = 0.701 m and h_1 = 0.617 m). Figure 12 reveals that M_a is much larger than $M_{t0.65}$, and close to $M_{t0.82}$. And the deviation between $M_{t0.65}$ and $M_{a-20\%}$ is slightly separated when tank body is continuously released by hole 2 (d = 0.0034 m, h = 0.701 m and h_1 = 0.4677 m). Figure 13 demonstrates that M_a is much larger than $M_{t0.65}$ but much closer to $M_{t0.82}$.

Furthermore the deviation between $M_{t0.65}$ and $M_{a-20\%}$ is almost the same when the tank body is continuously released by hole 3 (d = 0.0033 m, h = 0.701 m and h_1 = 0.2677 m).

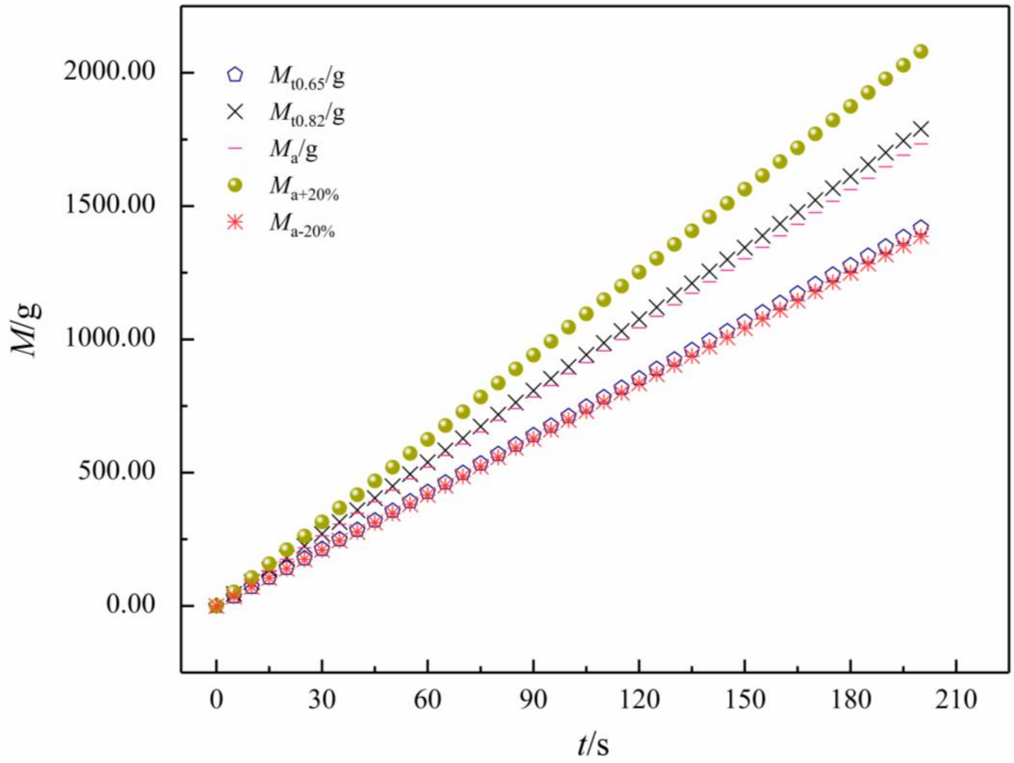

Figure 11. Deviation leakage curves of hole 1 with time (d = 0.0033 m, h = 0.701 m and h_1 = 0.617m).

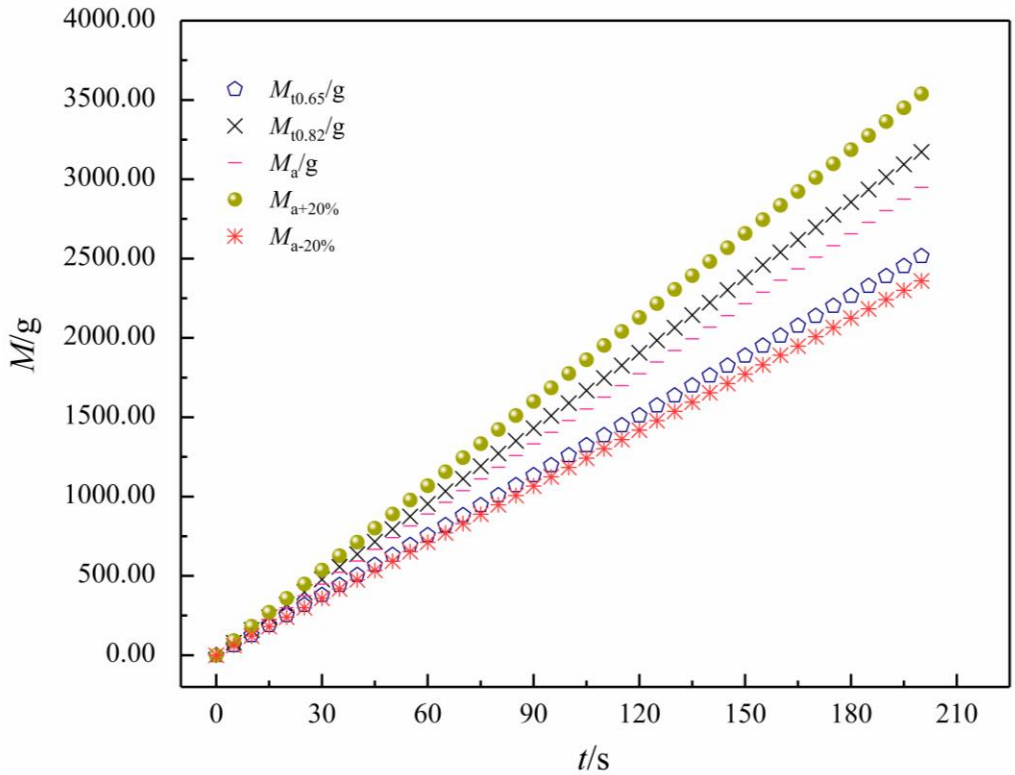

Figure 12. Deviation leakage curves of hole 2 with time (d = 0.0034 m, h = 0.701 m and h_1 = 0.4677m).

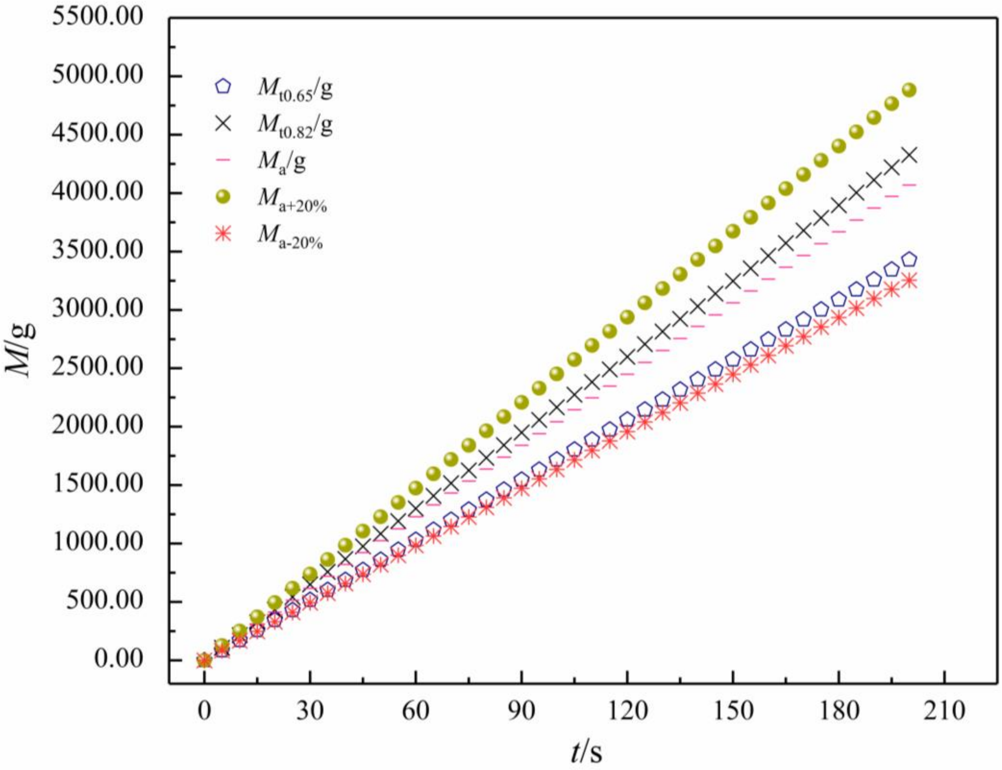

Figure 13. Deviation leakage curves of hole 3 with time (d = 0.0033 m, h = 0.701 m and h_1 = 0.2677 m).

Discharge coefficient C_0 is an important factor for calculation of theoretical leakage amount. $C_{0,}$ as a theoretical discharge coefficient, is more suitable for the value of 0.82 under the condition studied in this paper. Figure 14 gives the relationship between M_a and M_t for leaking hole 1, 2 and 3. It could be straightly seen that the curves of M_a and $M_{t0.82}$ are almost completely coincident, which demonstrates that theoretical value of 0.82 for discharge coefficient C_0 is perfect for hole 1 (d = 0.0033 m, h = 0.701 m and h_1 = 0.617 m). The curves of M_a and $M_{t0.82}$ have a little overlap, which states that theoretical discharge coefficient C_0 should be corrected for hole 2 (d = 0.0034 m, h = 0.701 m, h_1 = 0.4677 m). The curves of M_a and $M_{t0.82}$ have a slightly gap, which demonstrates that theoretical discharge coefficient C_0 is 0.82 and could be used for hole 3 (d = 0.0033 m, h = 0.701 m and h_1 = 0.2677 m).

Consequently, the real–time leakage amount shows good linearity within 200 s leakage time. It can be seen that $M_{t0.65}$ for leakage hole 1 is very close to the average deviation $M_{a–20\%}$ of the experimental leakage amount, while the M_t for leakage hole No. 2 and No. 3 have a certain deviation from $M_{a–20\%}$. All the M_a of three holes are less than its $M_{t0.82}$ but closely to its $M_{t0.82}$, which demonstrates the validity of the model.

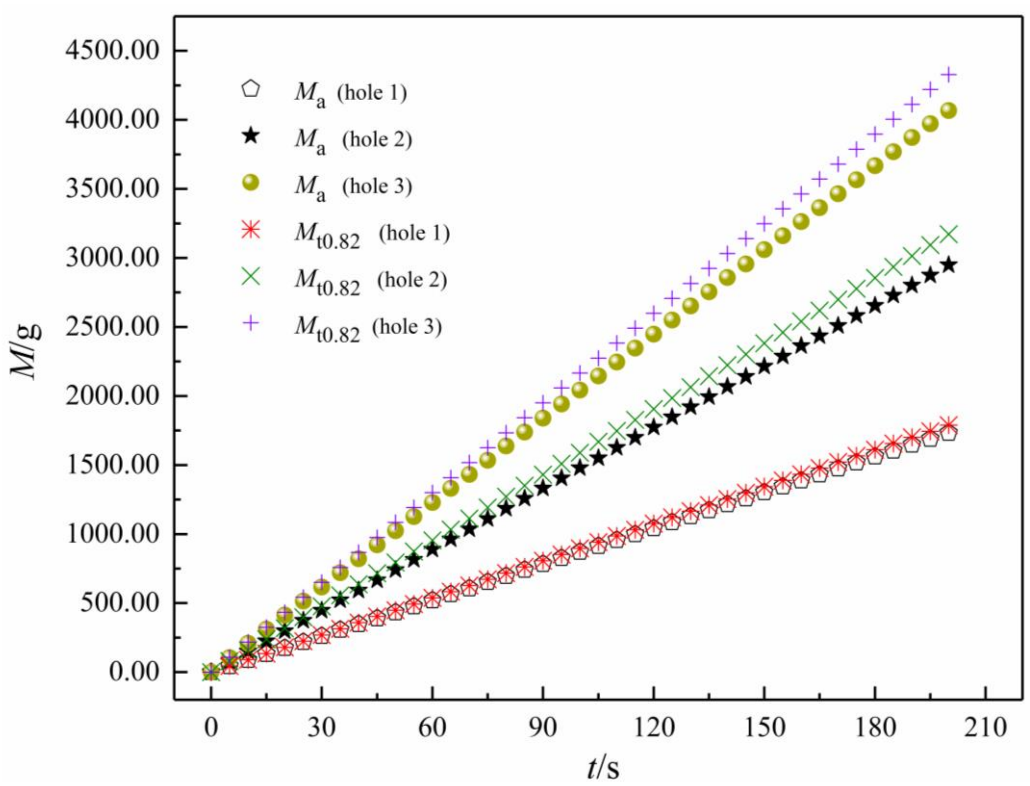

Figure 14. M_t and M_a relationship of leakage hole 1, 2 and 3.

4.2.2. Effect of Liquid Level above the Leak Hole on Leakage Stability

The effect of the liquid level above the leak orifice on the leak hole is mainly reflected in the pressure at the leak hole. Under the same meteorological conditions, the pressure at the leakage hole is $P - P_0 + \rho g h_L$ when the original liquid level h in the storage tank is unchanged and the distance between the leakage hole and the ground h_1 is different. The pressure at the leak hole is $\rho g h_L$ because the liquid saturated vapor pressure ($P - P_0$) is negligible for the regular pressure tank. The experimental leak amount M of different leak holes varies with the instantaneous continuous flow velocity at the leak hole changes because of the pressure.

The liquid level height h_L above the leakage hole increases as the height h_1 of the leakage hole decreases, the liquid level change Δh in the storage tank will decrease slowly after the leakage occurs when the original liquid level h is unchanged, so the change of pressure generated ($\rho g h_L$) is small. Therefore, the smaller the height h_1 of the leakage hole is, the more stable the instantaneous continuous flow velocity is and the larger leakage rate is. Obviously, during any time of the leakage, the real–time leakage amount M_a of the *N*o. 1 hole is the smallest, while the M_a for the No. 3 hole is the largest (Figure 14). This is verified by leak test data for holes NO. 1, 2 and 3.

4.2.3. Effect of Discharge Coefficient C_0 on Leakage

The discharge coefficient C_0 represents the dimensionless constant [27], which is obtained from the complex function of the Reynolds number of the flow and the leak bore diameter [5, 28, 29, 30, 31]. The Reynolds number is defined as $Re = \rho v d / \eta$, where ρ is the liquid density, v is the liquid flow rate at the leak hole, d is the release hole diameter, and η is the dynamic viscosity coefficient of the liquid. Because the discharge coefficient C_0 is affected by the Reynolds number and the diameter of the leakage hole, the flow velocity of the leakage orifice changes continuously due to these factors. The original liquid level h and the height h_1 are different from each other, which leads to the corresponding Reynolds number Re being different, so the discharge coefficient C_0 is a non – constant value. In summary. C_0 should be adjusted according to the situation. In this paper, C_0 is 0.82 for calculation of the theoretical leakage amount M_t.

5. Conclusions

This paper focuses on the calculation of continuous real–time leakage amount after liquid hazardous chemicals vertical tank releases. Through mathematical modeling, programming the model, and experimental verification, the conclusions are obtained as follows:

(1) The mathematical model of continuous real–time release M and leakage time t is established by the principle of mass conservation, which can improve the accuracy of continuous real–time release in any leakage period after the tank body leaks.

(2) By experimental analysis of repeated leakage tests, the more stable the flow rate and the larger the leak rate are under the condition that the higher the liquid level above the leakage hole (h_L) is, the greater the pressure on the leak hole is and the smaller the pressure changes at the leaking hole is. All the M_a of three holes are less than its $M_{t0.82}$ but closely to its $M_{t0.82}$, the experimental results states that the established model is effective.

(3) The discharge coefficient (C_0) affects the accuracy of calculating leakage amount, which may lead to deviations between M_t and M_a. The calculation accuracy of the continuous real–time leakage amount M can be realized when the value of discharge coefficient is appropriate, and the reliability of early warning prevention scheme can be provided for enterprise and government emergency rescue.

Author Contributions: J. H., L. Y. and Y.Z. conceived the initial and final design of the research work. Q. Z., D. Z. and L.L. completed the experiments. A. L. simulated the model by C#. J. H. and D. Y. analyzed the results and finished the manuscript's preparation. J. H., L. Y. and Y.Z. discussed the work with the rest of the authors and refined the manuscript. J. H. wrote the paper with co-authors' support.

Funding: This study is supported by the key research and development program in Guangxi (category: *research and demonstration of key technologies for public safety and disaster prevention and mitigation*, Grant number: Guike AB16380288.

Acknowledgments: We would like to thank the anonymous reviewers for their time, work, and valuable feedback.

Conflicts of Interest: The authors declare no conflict of interest.”

Nomenclature

M	continuous real–time leakage amount	g
Q_m	mass flow	kg/s
Q_v	volume flow	m^3/s
ρ	liquid density	kg/m^3
A_1	bottom area of the tank	m^2
A	area of leaking hole	m^2
C_0	discharge coefficient	–

P	liquid pressure in the tank	Pa
P_0	environmental pressure	Pa
g	gravitational acceleration	$9.8 m/s^2$
h	original liquid height in the tank before leakage	m
h_1	distance from the leaking point to tank bottom	m
h_L	liquid height above the leaking hole	m
Δh	height at which the liquid level drops after the tank leaks	m
v	flow rate of the liquid at the leak hole	m/s
v_1	falling liquid level velocity in the tank	m/s
a_1	changing rate of the liquid level falling velocity in the storage tank	m/s^2
t	leakage time	s
C_1	internal constant	–
C_2	internal constant	–
V	total volume of liquid leaked	m^3
D	tank bottom diameter	0.98m
H	total tank height	1.45m
H_1	cylindrical part height	1.04m
d	leakage hole diameter	mm
M_1	continuous leakage amount of the first experiment of every hole	g
M_2	continuous leakage amount of the second experiment of every hole	g
M_3	continuous leakage amount of the third experiment of every hole	g
M_{a}	average amount of the three experimental leakage of every hole	g
M_{t}	theoretical leakage calculation of every hole	g
$M_{\mathrm{t}0.65}$	theoretical leakage calculation (C_0 = 0.65) of every hole	g
$M_{\mathrm{t}0.82}$	theoretical leakage calculation (C_0 = 0.82) of every hole	g
$M_{a+20\%}$	average value of the experimental leakage is positive by 20 %	g
$M_{a-20\%}$	average value of the experimental leakage is negative by 20 %	g
Re	Reynolds number	–
η	dynamic viscosity coefficient of the liquid	–

References

1. Cirimello, P. G., Otegui, J. L., Ramajo. D., et al. A major leak in a crude oil tank: Predictable and unexpected root causes. Eng. Fail. Anal. **2019**, 100, 456–469. https://doi.org/10.1016/j.engfailanal.2019.02.005.
2. Hu, K., Zhao. Y. Numerical simulation of internal gaseous explosion loading in large–scale cylindrical tanks with fixed roof. J. Thin–Walled Struct. **2016**, 105,16–28. http://dx.doi.org/10.1016/j.tws.2016.03.026.
3. S. M. Tauseef, Tasneem Abbasi, V. Pompapathi, S.A. Abbasi. Case studies of 28 major accidents of fires/explosions in storage tank farms in the backdrop of available codes/standards/models for safely configuring such tank farms. Process Saf. Environ. Prot. **2018**, 120, 331–338. https://doi.org/10.1016/j.psep.2018.09.017.

4. Li Yunhao, Jiang Juncheng, Zhang Qingwu, Yu Yuan, Wang Zhirong, Liu Haisen, Shu Chi–Min. Static and dynamic flame model effects on thermal buckling: Fixed–roof tanks adjacent to an ethanol pool–fire. Process Saf. Environ. Prot. **2019**, 127, 23–35. https://doi.org/10.1016/j.psep.2019.05.001.
5. CPD. Purple Book: Guideline for Quantitative Risk Assessment. Committee for the Prevention of Disasters, Hague, Netherlands, **2005**a.
6. CPD. Red Book: Methods for Determining and Processing Probabilities. Committee for the Prevention of Disasters, Hague, Netherlands, **2005**b.
7. CPD. Yellow Book: Methods for the Calculation of Physical Effects. Committee for the Prevention of Disasters, Hague, Netherlands, **2005**c.
8. Liu, Q., Chen, Z., Liu, H., et al.. CFD simulation of fire dike overtopping from catastrophic ruptured tank at oil depot. J. Loss Prev. Process Ind. **2017**, 49, 427–436. http://dx.doi.org/10.1016/j.jlp.2017.06.005.
9. Luo Tongyuan, Wu Chao, Duan Lixiang. Fishbone diagram and risk matrix analysis method and its application in safety assessment of natural gas spherical tank. J. Clean. Prod. **2018**, 174, 296–304. https://doi.org/10.1016/j.jclepro.2017.10.334.
10. Lu, J., Yang, Z., Wu, H., et al. Model experiment on the dynamic process of oil leakage from the double hull tanker. J. Loss Prev. Process Ind. **2016**, 43, 174–180. http://dx.doi.org/10.1016/j.jlp.2016.05.013.
11. Si, H., Ji, H., Zeng, X. Quantitative risk assessment model of hazardous chemicals leakage and application. J. Saf. Sci., **2012**, 50(7):1452–1461. https://doi.org/10.1016/j.ssci.2012.01.011.
12. He, B., Jiang, X. S., Yang, G. R., et al. A numerical simulation study on the formation and dispersion of flammable vapor cloud in underground confined space. Process Saf. Environ. Prot., **2017**, 107, 1–11. http://dx.doi.org/10.1016/j.psep.2016.12.010.
13. He, G., Liang, Y., Li, Y., et al. A method for simulating the entire leaking process and calculating the liquid leakage volume of a damaged pressurized pipeline. J. Hazard. Mater. **2017**, 332, 19–32. http://dx.doi.org/10.1016/j.jhazmat.2017.02.039.
14. He, J.X., Yang, L.L., Liu, B., et al. 07.04. A calculation model based on continuous real–time leakage of normal pressure vertical storage tank body. Application number of Chinese patent CN 201810724745.0. **2018**. http://www.soopat.com/Patent/201810724745.
15. Zhen, X., Vinnem, J, E., Peng, C., et al., 2018. Quantitative risk modelling of maintenance work on major offshore process equipment. J. Loss Prev. Process Ind. **2018**, 56, 430–443. https://doi.org/10.1016/j.jlp.2018.10.004.
16. DNV. UDM Verification Manual. DNV Software, UK, **2006**.
17. DNV. PHAST Software Introduction [Online], Available: https://www.dnvgl.com/services/hazard–analysis–phast–1675, **2016**.
18. Dennis P. Nolan. Handbook of Fire and Explosion Protection Engineering Principles (Third Edition). Dennis P. Nolan, **2014**, 247–252.
19. Santiago Zuluaga Mayorga, Mauricio Sánchez–Silva, Oscar J. Ramírez Olivar, Felipe Muñoz Giraldo. Development of parametric fragility curves for storage tanks: A Natech approach. Reliab. Eng. Syst. Saf. **2019**, 189,1–10. https://doi.org/10.1016/j.ress.2019.04.008.
20. China Coal Industry Publishing House, 2013. Guidelines for Quantitative Risk Assessment of Chemical Enterprises (AQ/T 3046 – 2013), Beijing, **2013**.
21. Kasai, N., Maeda, T., Tamura, K., et al.. Application of risk curve for statistical analysis of backside corrosion in the bottom floors of oil storage tanks. Int. J. Pres Ves Pip, **2016**, 141:19–25. http://dx.doi.org/10.1016/j.ijpvp.2016.03.014.

22. Shokrzadeh, A, R., Sohrabi, M, R. Buckling of ground based steel tanks subjected to wind and vacuum pressures considering uniform internal and external corrosion. J. Thin Wall Struct. **2016**, 108, 333–350. http://dx.doi.org/10.1016/j.tws.2016.09.007.
23. Amir R. Shokrzadehn, Mohammad R. Sohrabi.. Buckling of ground based steel tanks subjected to wind and vacuum pressures considering uniform internal and external corrosion. Thin–walled Struct., **2016**, 108, 333–350. http://dx.doi.org/10.1016/j.tws.2016.09.007.
24. Manshadi S H D, Maheri M R. The effects of long–term corrosion on the dynamic characteristics of ground based cylindrical liquid storage tanks. Thin–Walled Struct. **2010**, 48(12): 888–896. http://dx.doi.org/10.1016/j.tws.2010.05.003.
25. Mariusz Maslaka1, Michal Pazdanowskia, Janusz Siudutb, Krzysztof Tarsac. Corrosion durability estimation for steel shell of a tank used to store liquid fuels. Procedia Engi. **2017**, 172, 723–730. http://dx.doi.org/10.1016/j.proeng.2017.02.092.
26. Jiang, J.C. Accident Investigation and Analysis Technology, second ed. Chemical Industry Press, Beijing, **2011**.
27. Crowl D A. Liquid discharge from process and storage vessels. J. Loss Prev. Process Ind. **1992**, 5(2):73–80. https://doi.org/10.1016/0950–4230(92)80003.
28. DNV. DISC Theory Document. Palace House, 3 Cathedral Street, London SE19DE, UK, **2015**. http://www.dnv.com/software.
29. Masahiro Ishibashi. Discharge coefficient equation for critical–flow toroidal–throat venturi nozzles covering the boundary–layer transition regime. Flow Meas. and Instrum., **2015**, 44:107–121. http://dx.doi.org/10.1016/j.flowmeasinst.2014.11.009.
30. Reader–Harris M. J., Sattary J. A.. The orifice plate discharge coefficient equation. Flow Meas. and Instrum., **1990**, 1(2):67–76. https://doi.org/10.1016/0955–5986(90)90031–2.
31. S. Essien, A. Archibong–Eso, L. Lao. Discharge coefficient of high viscosity liquids through nozzles. Exp. Therm Fluid Sci., **2019**, 103 :1–8. https://doi.org/10.1016/j.expthermflusci.2019.01.004.